

We are IntechOpen, the world's leading publisher of Open Access books Built by scientists, for scientists

6,900

Open access books available

186,000

International authors and editors

200M

Downloads

Our authors are among the

154

Countries delivered to

TOP 1%

most cited scientists

12.2%

Contributors from top 500 universities



WEB OF SCIENCE™

Selection of our books indexed in the Book Citation Index
in Web of Science™ Core Collection (BKCI)

Interested in publishing with us?
Contact book.department@intechopen.com

Numbers displayed above are based on latest data collected.
For more information visit www.intechopen.com



Design, Performance, and Optimization of the Wire and Tube Heat Exchanger

I Made Arsana and Ruri Agung Wahyuono

Abstract

The wire and tube heat exchanger has been mostly utilized as a condenser unit in various refrigeration systems. As a class of extended surface-based heat exchanger, not only the operating condition but also the geometry of the wire and tube heat exchanger plays a critical role in determining the overall performance of the heat exchanger. Despite the fact that the current designs that include the inline, single-staggered, and woven matrix-based wire and tube heat exchangers already exhibits positive performance, future design and optimization remain challenging from the thermal and fluids engineering point of view. To guide the optimization strategy in the heat exchanger design, this chapter provides an insight into how the geometrical design impacts the performance of various wire and tube heat exchangers, which can be deduced from either the heat exchanger capacity or efficiency.

Keywords: heat transfer, extended surface, operating condition, heat exchanger capacity

1. Introduction

The world is recently demanding the energy-efficient technology and process including in industry, building, and urban housing. Among various vital technologies, particularly in building and housing, the heat exchanger is one of the common technologies applied in, for example, air conditioners and refrigeration system. For these applications, it is common that the finned tube heat exchangers have been used [1, 2]. Particularly for the refrigeration system, the wire-based fin has been employed in the so-called wire and tube heat exchanger (or wire-on-tube heat exchanger). This wire and tube heat exchanger consists of a tube coil with certain spacing attached with small diameter wires acting as its extended surface [1–3]. The working fluid, for example, refrigerant, nanofluids, or thermal oil, flows inside the tubes, while the ambient air is exposed across the outside surface of the wire-attached tube coils, which allows for either natural or forced convection to dissipate the heat from the surface [1–5].

There have been many literatures reporting the thermal performances of wire and tube heat exchanger. The seminal work has been reported by Witzell and Fontaine [6, 7] who have investigated the thermal characteristic and the design procedure of wire and tube heat exchanger. Later, heat transfer modes of radiation

and natural convection from wire-on-tube heat exchanger have been studied in which the radiation considers all interactions between the surface and the surrounding environment [8]. Following this experimental study, some refrigeration research aiming at formulating the correlation on the air-side heat transfer coefficient in natural convection-based wire and tube heat exchanger has developed, including for a single-layer and a multiple-layer wire and tube [9–12], oscillating heat tubes [13], and wire-woven heat exchanger [14].

Recently, optimizing the wire and tube heat exchanger design into more compact geometry that exhibits high-heat exchanger efficiency and enables reduction the manufacturing cost. As it has been largely used as a condenser in the refrigeration system, reducing the size and material mass while showing high-specific cooling capacity is desirable for optimization. To do so, various numerical thermal models of wire and tube heat exchanger, which are mainly simulated using the finite element methods, have emerged in the last two decades allowing for a comprehensive analysis of the heat transfer process in the heat exchanger [15–19]. The emergence of these numerical studies is indicative of the current research direction on the development of wire and tube heat exchanges. Furthermore, numerical studies will serve as a versatile tool to analyze the performance of the wire and tube-based condenser for various geometrical design parameters, such as wire and tube spacing (pitch), wire and tube diameter, and operating conditions, such as mass flow rate and inlet temperature. It is also important to note that numerical studies will help to reduce the cost of testing and prototyping of modified wire and tube heat exchanger architecture.

In general, in spite of the currently available wire and tube heat exchanger working efficient and reliable, there is always a room for improvement toward optimum heat exchanger design, which is more efficient in terms of thermal efficiency, material mass, and manufacturing cost [16, 17]. It is prevalent that the design optimization using experimental approaches provides an actual figure of the heat exchanger performance. Nonetheless, as mentioned earlier, fabricating geometry-modified wire and tube heat exchanger will cost a considerable amount of money. Therefore, this chapter discusses how the design optimization can be carried out by minimizing effort in the experimental approach and maximizing the use of the experimentally validated numerical model. In this chapter, a custom-built heat exchanger testing apparatus will be presented and used to evaluate the thermal performance of wire and tube heat exchanger. Finite element methods using MATLAB programming and computational fluid dynamics (CFD) approach will be used for the optimization of the geometrical design as well as the operating condition and for understanding the physical phenomena underlying the heat transfer process in the heat exchanger, respectively.

2. Experimental approach

To explore the effect of geometrical design on the wire-tube configuration, three different configurations including inline, single-staggered, and woven matrix wire and tube heat exchanger were fabricated [20]. The design of wire and tube heat exchanger considered various geometrical aspects that include the width (W) of the wire cross, the wire length (L_w), the wire pitch (p_w), the wire diameter (D_w), the tube pitch (p_t) or tube spacing (s_t), and the tube diameter (D_t). The wire pitch then defined the number of wires used in a certain width of tube coil width (W). As shown in **Figure 1** (top and side view), the wire-tube connections were different among these three configurations and this difference was expected to affect the heat exchanger performance.

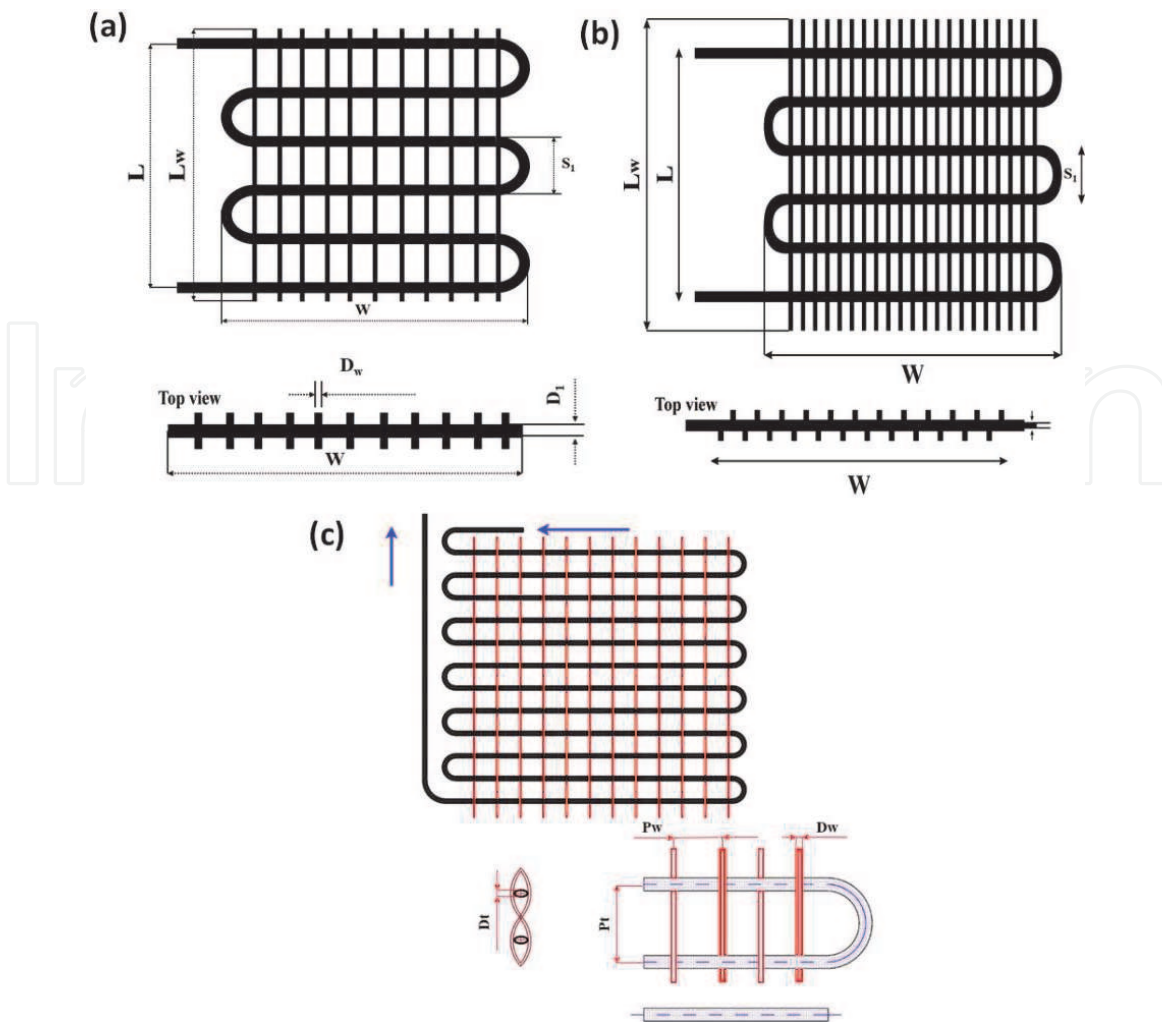


Figure 1. The wire and tube heat exchanger fabricated and tested in this study with (a) in-line, (b) single-staggered, and (c) woven matrix wire-tube configuration. Figure was adapted from Ref. [20] with permission.

The evaluation of heat exchanger capacity and efficiency employed the custom-built heat exchanger testing apparatus as shown in **Figure 2a** [20, 21]. Hot fluid was pumped through the wire and tube heat exchanger, on which the surface temperature was monitored at nine different selected positions. The mass flow rate, pressure, and temperature before and after passing through heat exchangers were monitored as well. Details on the components of the heat exchanger testing apparatus are described in **Figure 2b**, and the specification is summarized in **Table 1**.

2.1 Experimental test for evaluating the wire and tube heat exchanger performance

Running the experiment was started by soaking the working fluid, that is, oil Thermo 22, into the thermostatic vessel. It is worth noting that the apparatus was placed at constant room temperature (T_{∞}). Afterward, the pump was turned on allowing for the cold fluid to flow in the piping and tubing system. At this juncture, if there was no leakage, the pump was then turned back off. To manipulate the inlet fluid temperature, the working fluid was heated by the installed electric heater inside the vessel, and the temperature was controlled at the desired value. The pump again was turned on to circulate the heated working fluid. In addition, the inlet mass flow could be tuned by adjusting the opening of valves in the apparatus

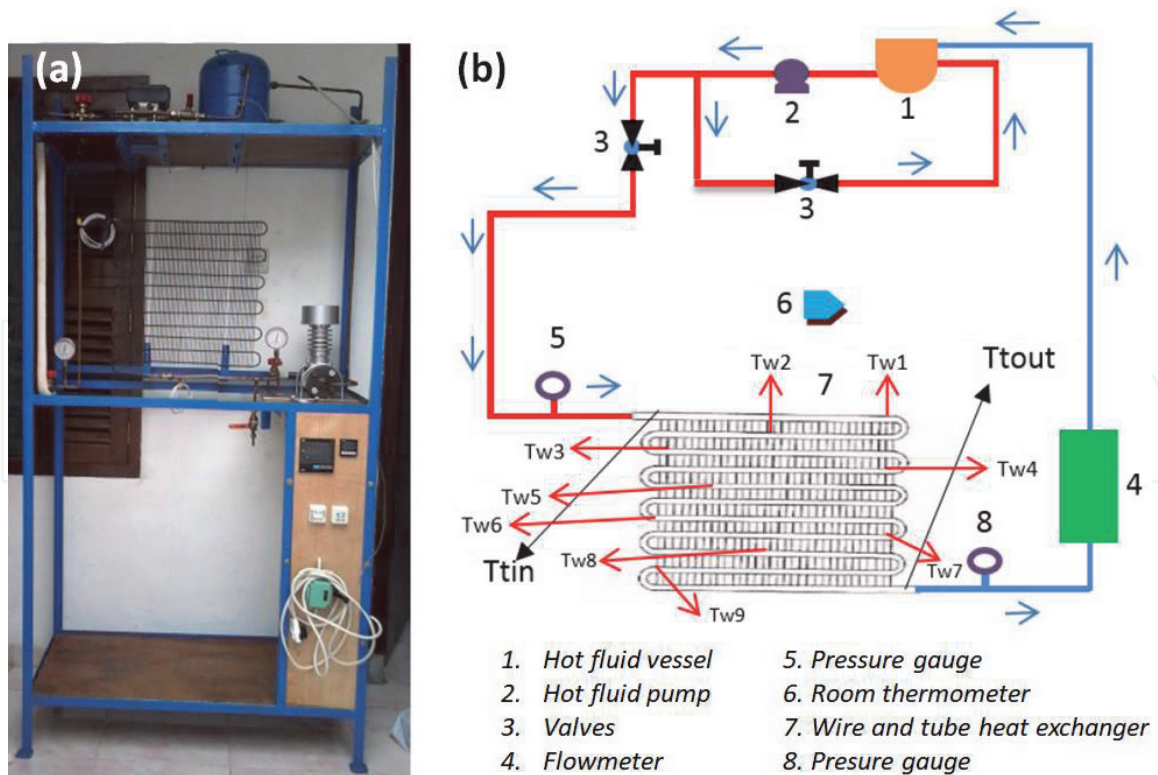


Figure 2. (a) The visual appearance of the heat exchanger testing apparatus, and (b) schematic of heat exchanger apparatus, which consists of thermostatic vessel embedded with electric heater, pump, pressure gauge, instrumentation box, flow meter, valves, and thermometer. Figure was adapted from Refs. [20,21] with permission.

No.	Component	Specification and operating condition
1	Hot fluid vessel	Atmospheric vessel (1 atm)
2	Hot fluid pump	Trochoid pump (Lamborghini, Italy)
3	Heating System	Thermo-controller: <ul style="list-style-type: none"> • PXR-9 (Fuji, Japan) • Range: 0–1000°C Thermocouple: <ul style="list-style-type: none"> • Fluks • Range: 0–200°C Heating element: <ul style="list-style-type: none"> • Lasco (Germany) • Power: 500 W
4	Flow meter	<ul style="list-style-type: none"> • Working fluid: oil • Accuracy: 0.1 kg cm⁻³ • Range: 30–100 lpm
5	Pressure gauge	<ul style="list-style-type: none"> • Zenit & Imperial • Accuracy: 0.2 kg cm⁻² • Range: 0–5 kg cm⁻²

Table 1. The specification and operating conditions of each component in the home-built heat exchanger testing apparatus [20–24].

and checked at the flow meter, which has an accuracy of 0.1 kg cm⁻³. During the experiment, wire-tube temperatures at nine different points ($T_{w1} - T_{w9}$ shown in **Figure 2b**), the inlet (T_{in}), and outlet (T_{out}) fluid temperature were recorded [22, 23].

2.2 Equations of convection

To evaluate the resulting experimental data, the air properties including density (ρ), kinematic viscosity (ν), Prandtl number (Pr), conduction coefficient (k), thermal diffusivity (α) were interpolated for every T_{out} . These properties were then used to determine the Grashof number (Gr), Rayleigh number (Ra), and Nusselt number (Nu) using the following equation:

$$Gr = \frac{g \cdot \beta \cdot (T_s - T_\infty) \cdot L^3}{\nu^2} \quad (1)$$

$$Ra = \frac{g \cdot \beta \cdot (T_s - T_\infty) \cdot L^3}{\nu \alpha} \quad (2)$$

$$Nu = \frac{4}{3} \left(\frac{Gr}{4} \right)^{0.25} \cdot f(Pr) \quad (3)$$

$$f(Pr) = \frac{0.75\sqrt{Pr}}{(0.609 + 1.221\sqrt{Pr} + 1.238Pr)^{0.25}} \quad (4)$$

The heat transfer coefficient was then calculated as follows:

$$h = \frac{Nu \cdot k}{L} \quad (5)$$

The heat exchanger capacity (Q) was then calculated based on the heat transfer coefficient in Eq. (5) using the following formula:

$$Q = h \cdot A \cdot (T_s - T_\infty) \quad (6)$$

where A is the total effective area of the wire and tube heat exchanger.

3. Numerical model to evaluate and to optimize the wire and tube heat exchanger performance

Numerical model in this chapter will be discussed based on the two approaches, that is, the finite element method (FEM) whose program was developed and run using a MATLAB program [24, 25] and the FEM using ANSYS Fluent for the computational fluid dynamics (CFD) approach [25–27]. For the FEM developed in MATLAB, the finite element was modeled as wire-tube element which is shown in **Figure 3**. Each modeled element is comprised of a tube whose length is equal to the wire pitch (pw) and the wire, which acts as a fin was set to have a length as long as the tube spacing or pitch (pt). The thermophysical properties of the fluid, which includes mass flow, temperature, enthalpy, and heat, were spatially calculated at the position of x and $x + dx$ for each element, where $dx = pw$.

The heat transfer in each element from the working fluid inside the tube to the surrounding air followed:

$$Q_{el} = UA_{el}(T_f - T_\infty)_{el} \quad (7)$$

where the conductance variable UA_{el} of each element was equal to $\frac{1}{R_i + R_t + R_o}$, and the thermal resistance of each wire-tube element could be expressed:

$$R_{w\&t} = \left(\frac{1}{h_i A_i} + \frac{\ln(r_o/r_i)}{2\pi k \Delta z} + \frac{1}{h_o A_o} \right)_{el} \quad (8)$$

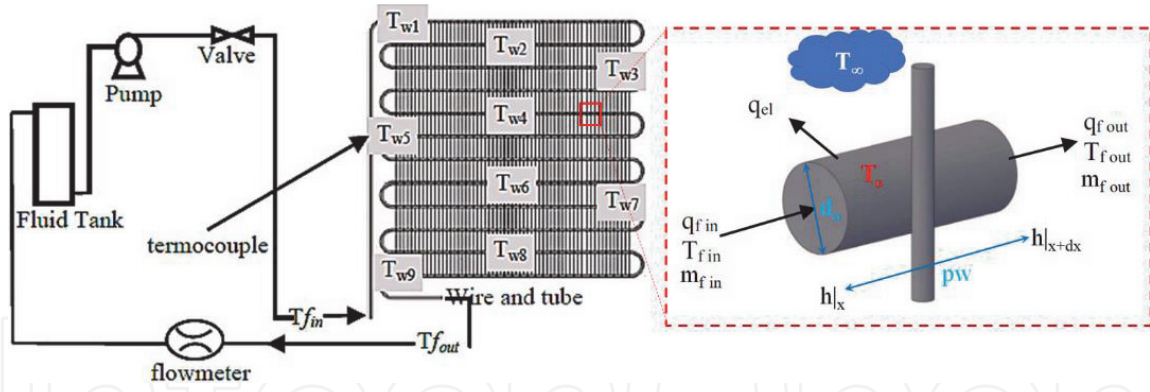


Figure 3.

The schematic of the wire-tube element to build finite element model for wire and tube heat exchanger.

The thermal resistance formula was used as a basis to calculate the convective heat transfer from the fluid to the tube wall, conduction inside the tube wall, and convection from the tube surface to the surrounding air. The area of each element was then determined as $A_o = A_t + A_w = \pi \cdot d_{t,o} \cdot p_w + 2 \cdot \pi \cdot d_w \cdot p_t$. As each element of the heat exchanger was extended by a wire-based fin, the wire efficiency could be calculated as follows:

$$\eta_w = \frac{\left[\tanh \left(\frac{m \times p_t}{2} \right) \right]}{\left[\left(\frac{m \times p_t}{2} \right) \right]} \quad (9)$$

in which it required convection and conduction heat transfer coefficient data to determine $m = \sqrt{\frac{Ah_w}{k_w d_w}}$. For initial calculation of the wire heat transfer coefficient, h_w was set to obtain $\eta_w = 0.9$. Assuming that the heat transfer coefficient is constant along with the wire element and the difference between the fluid temperature and the tube temperature is 0.5°C , the wire temperature was determined as follows:

$$T_w = \eta_w (T_{t,o} - T_\infty) + T_\infty \quad (10)$$

The average external (outer surface) temperature of each element could then be calculated as follows:

$$T_{\text{ex}} = \frac{(T_{t,o} + GP \cdot \eta_w \cdot (T_{t,o} - T_\infty) + GP \cdot T_\infty)}{(1 + GP)} \quad (11)$$

where GP is the geometrical parameter, $GP = 2 \left(\frac{p_t}{d_{t,o}} \right) \left(\frac{d_w}{p_w} \right)$. The heat transfer coefficient from the outer surface of the wire-tube element was determined from both free convection and radiation $h_o = h_c + h_r$ where the radiative heat transfer coefficient was defined as follows:

$$h_r = \varepsilon \cdot \sigma \cdot \frac{(T_{t,o}^4 - T_\infty^4)}{(T_{t,o} - T_\infty)} \quad (12)$$

To obtain the convective heat transfer coefficient $h_c = \frac{\text{Nu} \times k}{H}$, some dimensionless parameters, for example, Nusselt number (Nu) and Rayleigh number (Ra) have to be calculated:

$$\text{Nu} = 0.66 \left(\frac{\text{Ra} \cdot H}{d_{t,o}} \right)^{0.25} \left\{ 1 - \left[1 - 0.45 \left(\frac{d_{t,o}}{H} \right)^{0.25} \right] \exp \left(\frac{-s_w}{\phi} \right) \right\} \quad (13)$$

$$Ra = \left(\frac{\beta \rho^2 c p}{\mu k} \right)_a g(T_{t,o} - T_\infty) . H^3 \quad (14)$$

$$\phi = \left(\frac{28.2}{H} \right)^{0.4} s_w^{0.9} s_t^{-1.0} + \left(\frac{28.2}{H} \right)^{0.4} \left[\frac{262}{(T_{t,o} - T_\infty)} \right]^{0.5} s_w^{-1.5} s_t^{-0.5} p \quad (15)$$

$$s_t = \frac{(p_t - d_t)}{d_t} \quad (16)$$

$$s_w = \frac{(p_w - d_w)}{d_w} \quad (17)$$

Once the h_o was obtained, the h_o was compared to h_w . If the difference between h_o and $h_w > 0.1 \text{ W m}^{-2} \text{ K}^{-1}$, the h_o was set equal to h_w , and the calculation of h_i , h_o , and Q_{el} was run until the convergence criteria were satisfied. At the steady-state condition, the heat transfer from the fluid to the surrounding air was equal to the heat transfer from the fluid to the outer surface of the tube. Thus, the outer surface temperature of the tube, $T_{t,o}$, was determined as follows:

$$T_{t,o} = T_f - Q_{el} \left(\frac{1}{h_i A_i} + \frac{\ln(r_o/r_i)}{2\pi k l} \right)_{el} \quad (18)$$

The calculated $T_{t,o}$ was then compared to the initial $T_{t,o}$. If the error was more than 0.05°C , new $T_{t,o}$ was substituted into Eq. (11) and the program was run to satisfy the convergence criteria. The calculation resulted in the Q_{el} . For each element, the outlet fluid temperature was determined as follows:

$$T_{out} = \frac{Q_{el}}{\dot{m}} + T_{in} \quad (19)$$

where \dot{m} is the mass flow rate of the working fluid. The output of the i -th element will be used for the calculation for the $(i + 1)$ -th element until the last element of the wire and tube heat exchanger. The summation of all elements yielded Q_{tot} and the heat exchanger capacity was calculated using the following:

$$C = \frac{Q_{tot}}{\dot{m}} \quad (20)$$

The heat exchanger efficiency was determined from the ratio between the actual heat transfer rate to the heat transfer rate if all wire temperature = tube temperature. For heat exchanger temperature equal to the tube temperature, the heat exchanger efficiency followed:

$$\eta_{tot} = \frac{(\eta_w A_w + A_t)}{A_o} \quad (21)$$

For detailed simulation, the heat transfer process that was coupled with the fluid dynamics was modeled and solved using CFD Software package of ANSYS Fluent. Details of the step-by-step procedure of CFD can be found elsewhere [26, 27]. In this simulation, preprocessing, solving, and post-processing steps were respectively executed. The geometry of the wire and tube heat exchanger was modeled in a 1:1 geometric scale and meshed to create finite elements. Then, the boundary type and boundary condition of modeled geometry were defined. To solve the governing equations (the conservation of energy, mass conservation, and momentum), the initial condition of each boundary condition was inputted. The turbulence model used was Reynold-Average Navier-Stokes (RANS) $k-\omega$ SST (shear-stress transport).

This $k-\omega$ SST was used since it has a high stability in numerical calculation and could predict accurately the flow on adverse pressure gradient in boundary layer area [25].

4. Performance evaluation of the wire and tube heat exchanger with varying wire-tube configuration

Heat transfer process and its efficiency in the wire and tube heat exchanger are strongly dependent on the geometrical architecture between the wire and tube. In this section, the effect of wire-tube configuration, including inline, staggered, and woven matrix wire and tube, and the operating condition will be discussed based on the experimental investigation and numerical modeling using computational fluid dynamics (CFD).

4.1 The empirical efficiency formulation of the inline wire and tube heat exchanger

To have a starting point for further geometrical optimization, here the simple inline wire and tube heat exchanger is discussed. An experimental investigation using different wire geometries, that is, wire pitch to wire length ratio (pw/Lw), under different operating conditions, that is, inlet fluid temperature of 40–80°C with 10°C intervals, has been carried out [28]. As the heat exchanger has been tested in an isolated and air-conditioned room, the heat exchanger can be assessed employing the relevant parameters and the dimensional analysis to generate a dimensionless equation following the π -Buckingham theory. Thus, the heat exchanger efficiency follows:

$$\eta_o = \frac{q_t}{q_{max}} = \frac{h \cdot s_w (T_w - T_\infty) + h \cdot s_t (T_t - T_\infty)}{h \cdot s_{tot} (T_t - T_\infty)} \quad (22)$$

$$q_t = f[q_{max}, g, \beta, \alpha, v, \Delta T, pw, dw, Lw, pt, dt] \quad (23)$$

The above function can be grouped into several dimensionless parameters: $\pi_1 = \frac{q_t}{q_{max}} = \eta_o$ is the heat exchanger efficiency, $\pi_2 = \frac{g L w^3}{v^2}$ and $\pi_3 = \Delta T \cdot \beta$ are the Grashof number parameters, $\pi_4 = \frac{\alpha}{v}$ is the reciprocal of Prandtl number, $\pi_5 = \frac{pw}{Lw}$ is the dimensionless wire pitch, $\pi_6 = \frac{dw}{Lw}$ is the dimensionless wire diameter, $\pi_7 = \frac{pt}{Lw}$ is the dimensionless tube pitch, and $\pi_8 = \frac{dt}{Lw}$ is the dimensionless tube diameter. The equation can then be reformulated as follows:

$$\pi_1 = f \left[\frac{\pi_2 \cdot \pi_3}{\pi_4}, \pi_5, \pi_6, \pi_7, \pi_8 \right] \quad (24)$$

Considering that the wire diameter (dw), the tube diameter (dt), and the tube pitch (pt) are constant, the general mathematical expression of the heat exchanger efficiency can be written:

$$\eta_o = f \left[\frac{g \cdot \beta \cdot \Delta T \cdot L w^3}{v \cdot \alpha}, \frac{pw}{Lw} \right] \quad (25)$$

The above function suggests that the heat exchanger efficiency is a function of Rayleigh number (R_a) and the dimensionless wire pitch (or the wire pitch to wire length ratio (pw/Lw)).

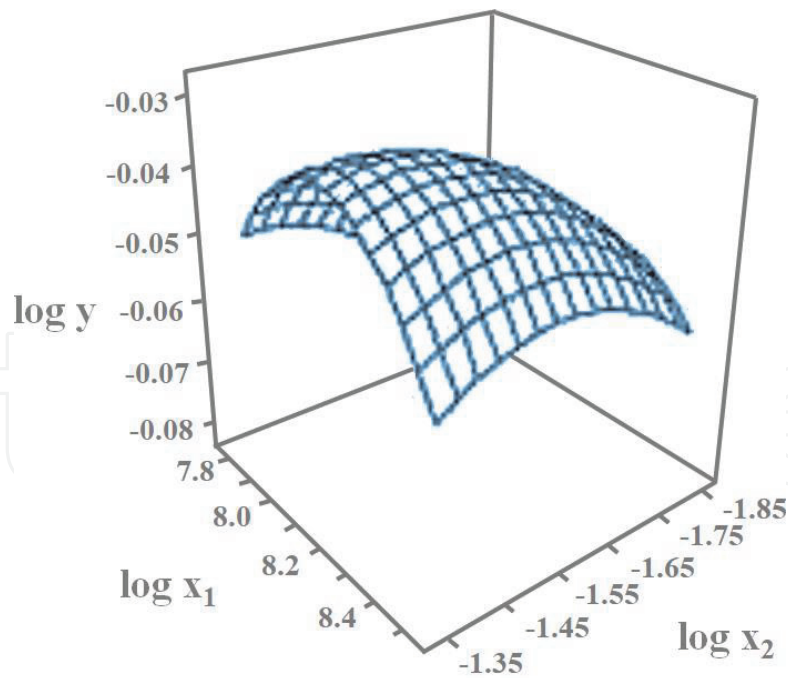


Figure 4. Contour plot of the heat exchanger efficiency ($\log y$) as a function of Rayleigh number ($\log x_1$) and wire geometry ($\log x_2$, where $x_2 = pw/Lw$). Figures from Ref. [28] used with permission.

Figure 4 shows the contour plot of the heat exchanger efficiency (y) as function of R_a (x_1) and the wire pitch to wire length ratio (pw/Lw) (x_2). Fitting the experimental data using multivariable logarithmic regression results in the best fitting parameter ($R^2 = 0.897$) with the resulting function as follows:

$$\begin{aligned} \log \eta_o = & -8.650 + 2.161 \log R_a + 0.259 \log \left(\frac{pw}{lw} \right) - 0.041 (\log R_a)^2 \\ & - 0.146 \left(\log \left(\frac{pw}{lw} \right) \right)^2 - 0.084 \left(\log R_a \times \log \left(\frac{pw}{lw} \right) \right) \end{aligned} \quad (26)$$

The above empirical formulation is considered a helpful finding to assist the heat exchanger optimization by taking into account both geometrical aspects of the wire-tube configuration and the operating condition, which is limited by the optimum R_a value ($\log^{-1}(x_1)$ at which the $\log y$ is maximum).

As above discussed quantitatively, the R_a is dependent on the Prandtl number and Grashof number, and hence, the inlet mass flow inlet as well as the inlet fluid temperature plays role in determining the heat exchange efficiency. To gain its qualitative and quantitative correlation between these operating conditions to the wire and tube heat exchanger efficiency, **Table 2** summarizes the heat exchanger capacity (Q) and heat exchanger efficiency (η) upon varying the inlet mass flow and temperature [22, 23]. In this investigation, the wire and tube heat exchanger possess the following specifications: wire length of 445 mm, wire pitch of 7 mm, wire diameter of 1.2 mm, tube diameter of 5 mm, tube pitch of 476 mm, and tube turn of 12.

At a constant inlet mass flow of $5 \times 10^{-3} \text{ kg s}^{-1}$, the heat exchanger performance improves with increasing inlet fluid temperature. As the temperature increases, the outer surface temperature of wire and tube heat exchanger increases, and hence, the overall heat transfer rate is enhanced, that is, the internal forced convection and conduction from the fluid to the wire-tube elements, and the external radiation from the surface to surrounding and the free convection. Meanwhile, at the same fluid inlet temperature of 70°C increasing the mass flow from $4 \times 10^{-3} \text{ kg s}^{-1}$ to

Wire and tube	Controlled parameter	Varied operating condition	Q (W)	η
In line (pw = 7 mm)	$M_{in} = 5 \times 10^{-3} \text{ kg s}^{-1}$	$T_{in} 50^\circ\text{C}$	9	0.47
		$T_{in} 60^\circ\text{C}$	19	0.65
		$T_{in} 70^\circ\text{C}$	24	0.66
In line (pw = 7 mm)	$T_{in} 70^\circ\text{C}$	$m_{in} = 4 \times 10^{-3} \text{ kg s}^{-1}$	33.27	0.67
		$m_{in} = 5 \times 10^{-3} \text{ kg s}^{-1}$	37.62	0.46
		$m_{in} = 6 \times 10^{-3} \text{ kg s}^{-1}$	41.17	0.73

Table 2.

Heat transfer capacity and heat exchanger efficiency for the inline wire and tube heat exchanger. Data are summarized from Refs. [22,23] upon permission.

$6 \times 10^{-3} \text{ kg s}^{-1}$ enhances the heat exchanger capacity by 24% and the efficiency also increases from 0.67 to 0.73. This increasing heat exchanger capacity is due to the higher mass flow in the tubes the higher the heat transfer rate to the surrounding colder air (at room temperature). This is simply reflected by the increasing inlet to outlet temperature difference ΔT , ($T_{in} - T_{out}$) which stems from the higher internal forced convection and external free convection as the mass flow increases.

4.2 Inline vs. staggered vs. woven matrix configuration

It is already mentioned that the wire is designed as an extended surface (fin) that is capable to enlarge the heat transfer area in the wire and tube heat exchanger. In this section, this wire-tube configuration will be the focus of the discussion. It is already known that inline and staggered wire and tube heat exchanger have been utilized quite extensively. Nonetheless, some experimentations on the development of woven matrix wire-tube configuration have emerged as it likely combines both the inline and staggered wire-tube configuration.

To compare the heat exchanger capacity among these wire-tube configuration, inline, single-staggered, and woven matrix wire and tube heat exchanger have been fabricated with a variation of wire pitch, that is, 7, 14, and 21 mm [21]. To gain deeper insight, the inlet fluid temperature also varied from 50 to 80°C with 10°C intervals. The heat exchanger apparatus was run at $2 \times 10^{-3} \text{ kg s}^{-1}$ inlet mass flow and the apparatus was placed in an air-conditioned room at 32°C. **Figure 5** displays the heat exchanger capacity of the wire and tube heat exchanger, which is affected by inlet fluid temperature, wire pitch, and the wire-tube configuration. In general, irrespective of the wire-tube configuration the heat exchanger capacity tends to increase with increasing inlet fluid temperature, whereas the heat exchanger capacity tends to decrease by enlarging the wire pitch irrespective of the wire-tube configuration. For 7 mm wire pitch (**Figure 5a**), inline configuration outperforms other configurations, which is plausible since for inline wire-tube configuration the number of wires used is larger than other configurations. This implies that the extended surface by the surface is enlarged, and thus, the heat transfer rate becomes more efficient.

It is interesting to note that the larger the wire pitch (see **Figure 5b** and **c**) the smaller the difference in heat exchanger capacity among three different wire-tube configurations. Particularly for 21 mm wire pitch, the heat exchanger capacity of a single-staggered configuration is on par with the inline configuration, in which the maximum heat exchanger capacity of 425 W is obtained at 80°C. The heat exchanger efficiency particularly for woven matrix wire and tube heat exchanger is shown in **Figure 5d**. An average of 69% heat exchanger efficiency is obtained

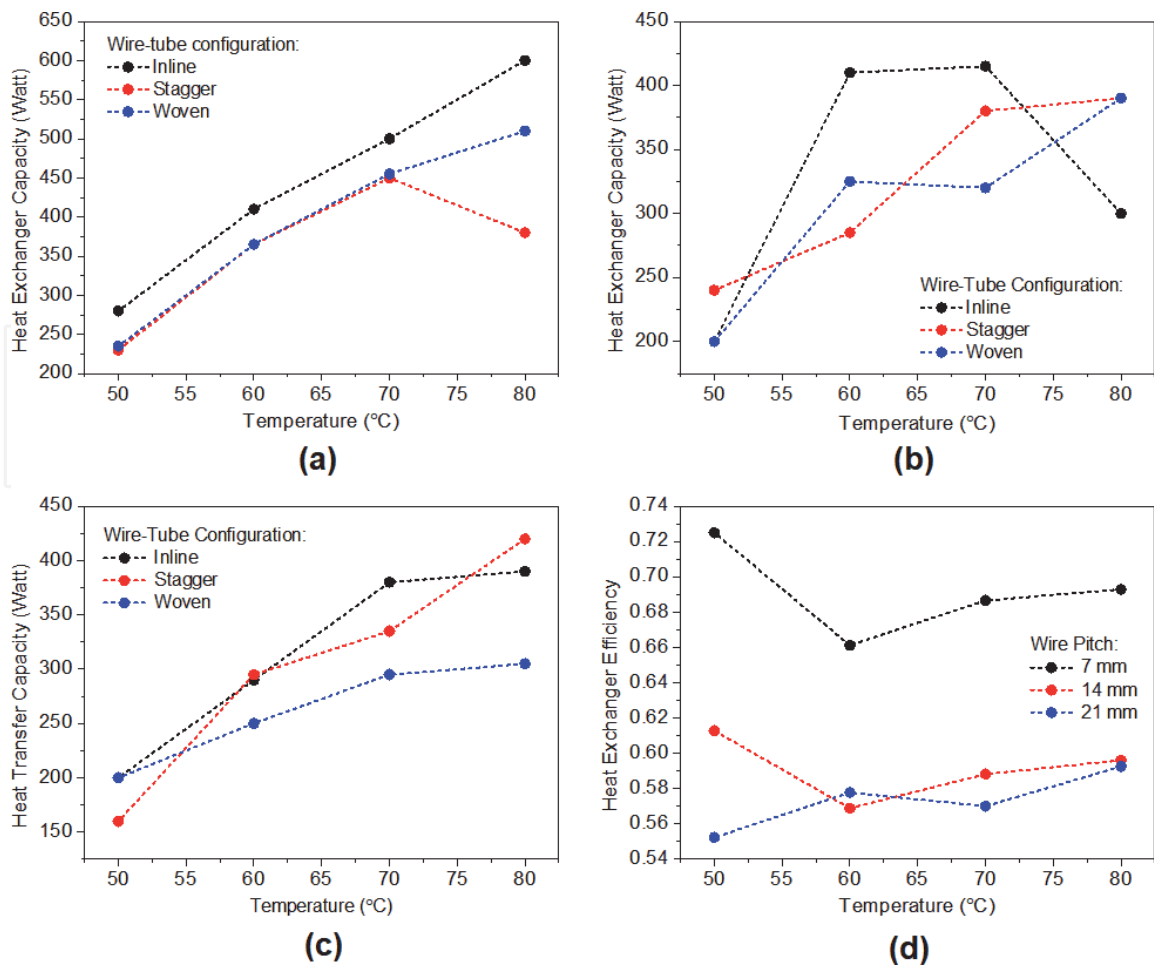


Figure 5. Different heat exchanger capacity of inline, single-staggered, and woven matrix wire and tube heat exchanger bearing pitch wire of (a) 7 mm, (b) 14 mm, and (c) 21 mm. (d) The efficiency of woven matrix wire and tube heat exchanger using different wire pitches and operated under varying inlet fluid temperature.

for 7 mm wire pitch, while the efficiency drops 10% down by changing the wire pitch to either 14 or 21 mm. This reflects that there is a room for optimization by varying the wire pitch between 7 mm and 14 mm.

Digging into the heat transfer process inside the wire and tube heat exchanger the change in the heat transfer coefficient is shown in **Figure 6** for the utilization of heat exchanger with 7 mm and 14 mm wire pitch. Irrespective of the wire pitch, it is clear that the convection heat transfer coefficient tends to decrease with increasing inlet fluid temperature. While larger wire pitch results in a larger heat transfer coefficient, the inline wire-tube configuration consistently yields the lowest heat transfer coefficient compared to a single-staggered and woven matrix wire-tube configuration. As the convection drops down while the heat exchanger increases at higher inlet fluid temperature, this implies that the conduction from the inner wall to the outer surface of the tube as well as wire tube and the radiation from the surface of the tube to the surrounding dominates the heat transfer process at a higher temperature.

5. Numerical model for heat exchanger performance prediction and optimization

As previously motivated in the introduction, a numerical model of the heat exchanger in general is developed to guide the future optimized design of the heat exchanger. Here, an example of a finite element model has been developed for a

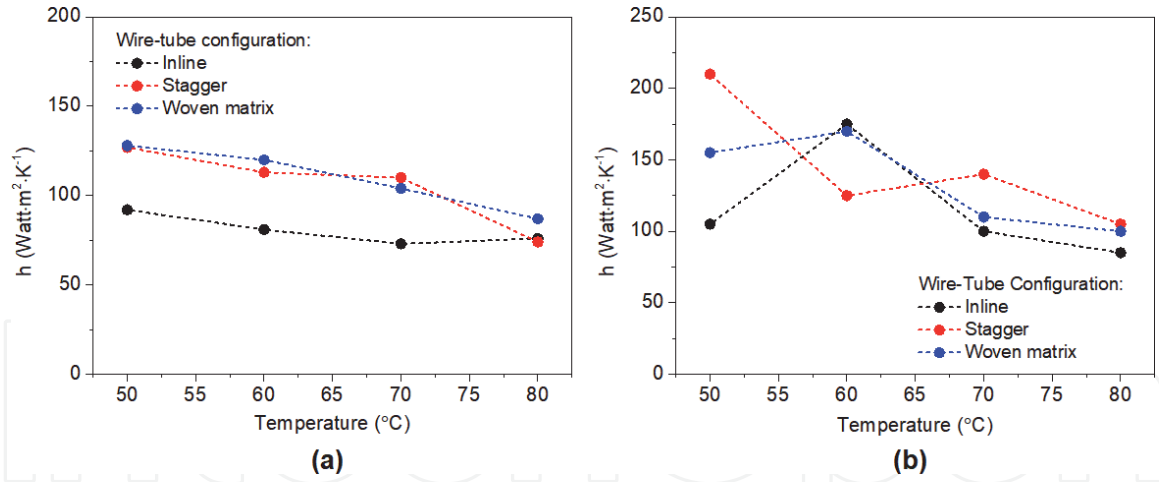


Figure 6. An exemplified of heat transfer coefficient h for the inline, single-staggered, and woven matrix wire and tube heat exchanger bearing pitch wire of (a) 7 mm and (b) 14 mm.

single-staggered wire and tube heat exchanger [24, 25]. In this case, the model was developed to aid the optimum design, which is limited by two variables including wire pitch (pw) and wire diameter (D_w). Experimental validation was carried out for the heat exchanger with wire pitch of 7 mm and 14 mm to assess the accuracy of the finite element model.

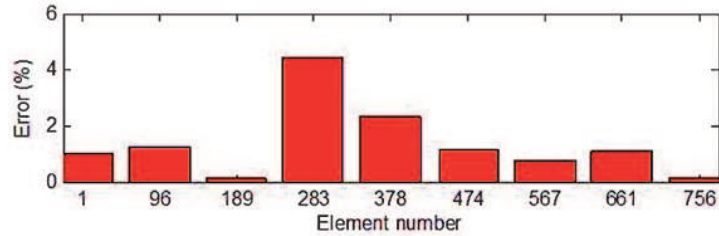
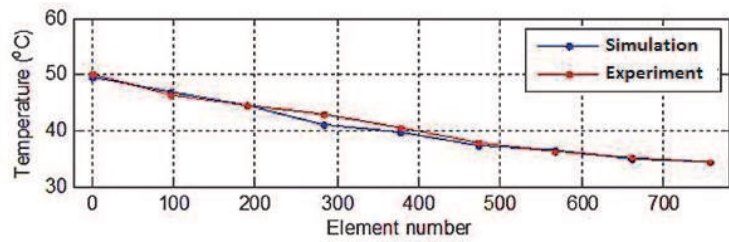
Figure 7 highlights the results of the finite element model on the single-staggered wire and tube heat exchanger using a wire pitch of 7 mm. The data verification reveals that the average error of modeling data compared to the measurement data is lower than 5%. In comparison, the earlier finding of the numerical simulation reported by Basal and Chin [16] that employed the heat load validation method yields an average error of up to 10%. This indicates that the simple finite element model developed in this work is considered reliable and accurate.

As the model is experimentally validated and reliable, this model was used to assess the heat exchanger capacity of the wire-tube configuration with the wire pitch spanning from 5 to 12 mm and the wire diameter spanning from 0.8 to 1.5 mm. The contour plot in **Figure 7b** displays the dependency of the heat exchanger capacity (Q_{tot}) to the wire pitch and diameter. For optimization procedure, an optimization factor (f) was defined:

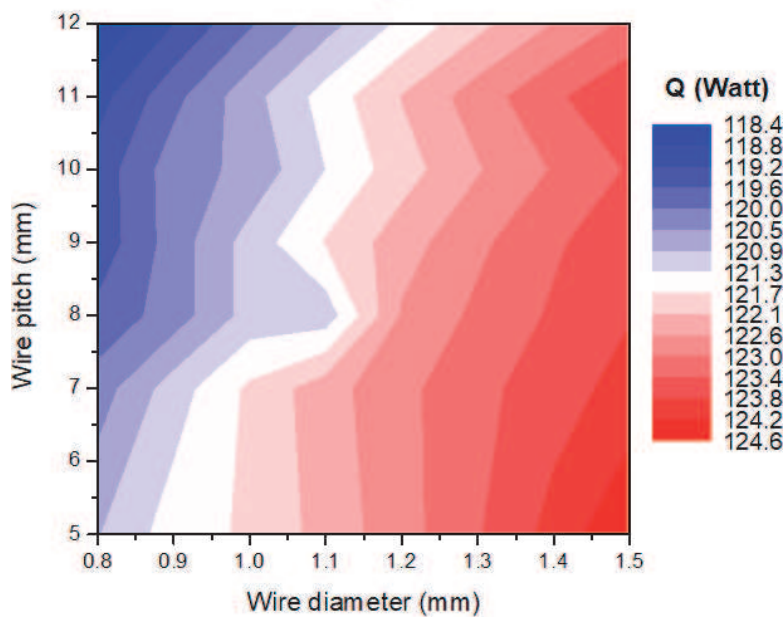
$$f = \frac{Q/W}{Q_0/W_0} \quad (27)$$

where Q is the capacity of the optimized heat exchanger, W is the mass of the heat exchanger, and Q_0 and W_0 are the capacity and mass of the basis designed heat exchanger, respectively.

In this case, the basis designed heat exchanger possess the following specifications: exchanger height of 445 mm; width of heat exchanger (wire) of 431 mm; width of heat exchanger (tube) of 476 mm; the tube length of 6416 mm; the outside tube diameter of 4.8 mm; the inside tube diameter of 3.2 mm; and the wire diameter of 1.2 mm. Using this consideration, the optimum condition is obtained if the optimization factor is maximum. In this regard, the optimum condition is obtained for Q_{tot} of 119.9214 W using a wire pitch of 11 mm and wire diameter of 0.9 mm. The contour plot in **Figure 7b** indicates that the smaller the wire pitch the bigger Q_{tot} . In addition, increasing the wire diameter tends to enhance the Q_{tot} . Nonetheless, if $pw \leq dw$, the system will merely be considered as tube, where the fins form of plate structure, and this condition yields lower Q_{tot} .



(a)



(b)

Figure 7.

(a) Temperature validation of each element for heat exchanger with wire pitch of 7 mm representing the wire temperature measured at nine measurement points. (b) Contour plot of the total heat exchanger capacity as a function of wire diameter and wire pitch. Figures from Ref. [24] used with permission.

Having optimized for the design of single-staggered wire and tube heat exchanger, the performance of inline and single-staggered wire-tube configuration is compared experimentally. The experimental data indicate that the inline configuration allows for 110 W heat release, while the single-staggered wire and tube heat exchanger exhibits a heat exchanger capacity of 107.3 W [24]. The difference is not that significant, and this result shows that changing the wire-tube geometry from inline to single-staggered already provides more efficient conditions. It is considered efficient as the single-staggered design reduces the number of wires used for manufacturing, and hence, it cuts the mass of construction materials and costs. Reducing the number of wires also leads to higher convective airflow since the flow is not blocked by the wall geometry as indicated from the velocity contour plot in **Figure 8**.

Figure 9a and **b** displays that air velocity distribution on the array of wire between inline and staggered heat exchanger. The results clearly indicate that the average velocity amplitude of the airflow around the wire tube is higher for a single-staggered one than that of the inline configuration. With velocity amplitude

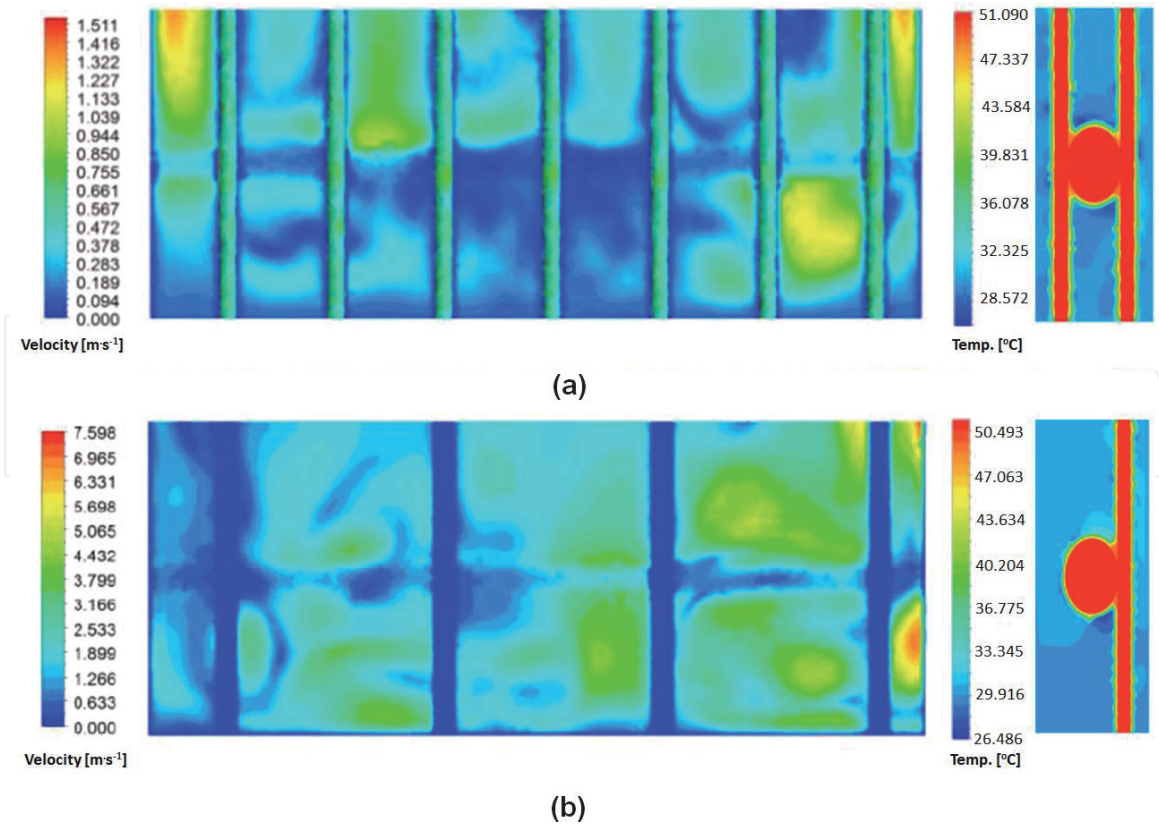


Figure 8. (Left) Velocity and (right) temperature contour of (a) inline and (b) single-staggered wire and tube heat exchanger bearing wire pitch of 7 mm. Figures from Ref. [24] used with permission.

of ~ 4 times higher and more homogeneously distributed, the single-staggered wire-tube heat exchanger also shows a slightly larger temperature difference between the outer surface of the wire-tube and the near-surface air. The more distributed air-flow in the vicinity of the staggered wire-tube configuration supports the argument that this configuration minimizes the airflow blocking by geometry wall. As the convective heat transfer coefficient is proportional to the air velocity, this leads to a higher rate of heat release by convection from the surface to the surrounding air.

It is already discussed that the numerical model is helpful to assist the optimization of a single-staggered wire and tube heat exchanger. Here, we further present the numerical study using CFD of single-staggered wire and tube heat exchanger with varying wire pitch (7, 9, and 11 mm) and inlet fluid temperature (40, 60, and 80°C) [26]. In this case, the inlet mass flow was set to $2 \times 10^{-3} \text{ kg s}^{-1}$. The simulation results show that the temperature difference ΔT ($T_{\text{in}} - T_{\text{out}}$) is exceptionally low and almost similar for the heat exchanger operated in the lowest inlet fluid temperature (**Figure 9a–c**). Thus, the inlet temperature of 40°C yields very low heat exchanger capacity irrespective of the wire pitch. **Figure 9d–f** exhibits quite significant ΔT upon increasing the inlet temperature to 60°C. For wire pitch of 7 mm, a $\Delta T = 26^\circ\text{C}$ is reached, while wire pitch of 9 and 11 mm shows ΔT of 24 and 22°C, respectively. This simulation is consistent with the experimental results that single-staggered wire and tube heat exchanger bearing 7 mm wire pitch shows $\Delta T = 26^\circ\text{C}$ [25, 26].

As we have noted previously that heat exchanger capacity tends to increase with increasing inlet fluid temperature, it is also obvious that at 80°C inlet temperature the ΔT becomes significantly higher. The ΔT magnitude for wire pitch of 7, 9, and 11 mm in heat exchanger operated at 80°C inlets are 30, 27, and 25°C, respectively. In brief, the CFD simulation allows for the prediction of the resulting ΔT and the

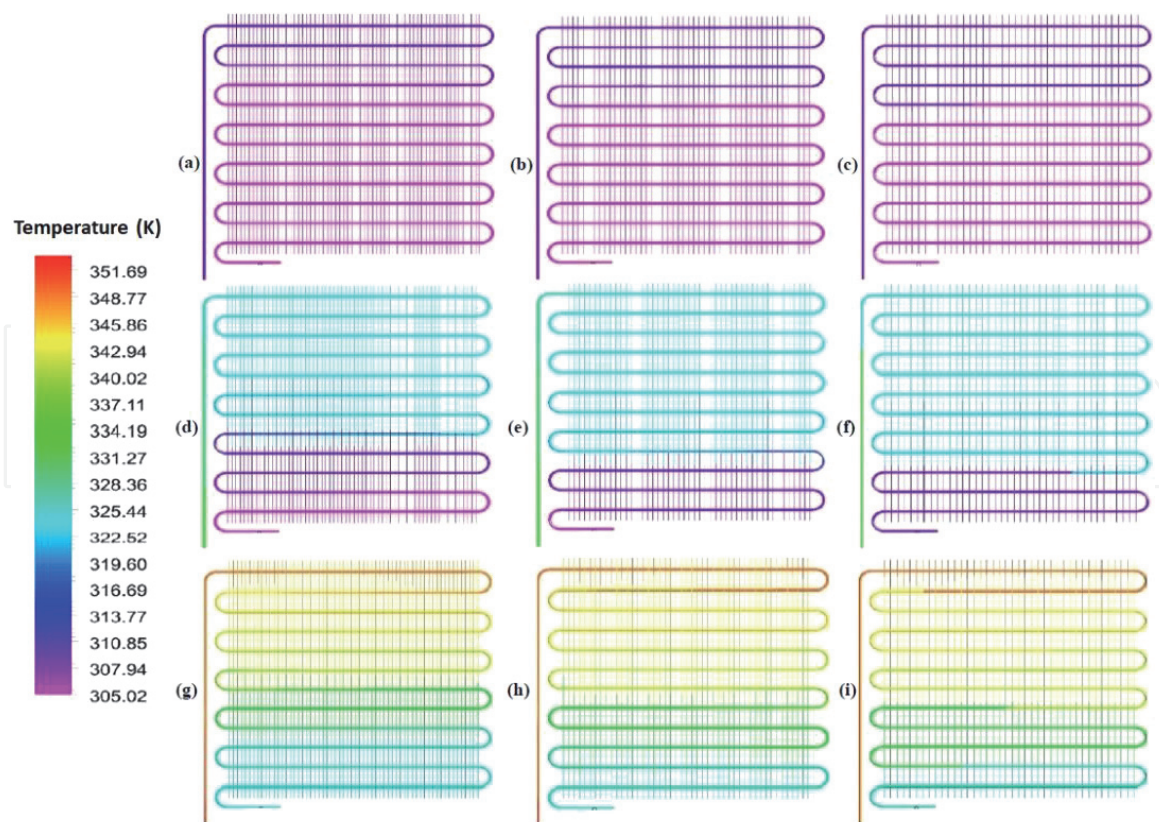


Figure 9. Temperature profile of the single-staggered wire and tube heat exchanger bearing wire pitch (p_w) of (a,d,g) 7 mm, (b,e,h) 9 mm, and (c,f,i) 11 mm operated using inlet fluid temperature of (top) 313 K (40°C), (middle) 333 K (60°C), and (bottom) 353 K (80°C). Figures from Ref. [26] used with permission.

average surface temperature of wire tube that can be used to evaluate heat exchanger capacity, wire efficiency as well as the heat exchanger efficiency.

Another set of examples benefitting the CFD approach for woven matrix wire and tube heat exchanger is shown in **Figure 10**. Previously, it is required for further optimization of woven matrix configuration with wire pitch below 14 mm. Thus, herein we discuss the performance of woven matrix wire and tube heat exchanger bearing wire pitch of 5, 7, and 9 mm and operated at different inlet mass flow, which was simulated using CFD [27]. In this case, the inlet temperature was set to 80°C. The general results show that lowering the mass flow rate from 1.10×10^{-3} to $0.55 \times 10^{-3} \text{ kg s}^{-1}$ increases the ΔT . For 5-mm wire pitch, a lower mass flow rate leads to outlet temperature as low as the ambient temperature (29.85°C). Similar results are obtained for heat exchanger bearing 7-mm wire pitch that can yield $\Delta T = 49.78^\circ\text{C}$ and outlet temperature of 30.4°C under the operating condition of $0.55 \times 10^{-3} \text{ kg s}^{-1}$ mass flow rate. Enlarging the wire pitch to 9 mm results in a lower heat transfer capacity as indicated by the higher outlet temperature even though the mass flow rate is set to the lowest. Considering that woven matrix wire and tube heat exchanger bearing wire pitch of 5 and 7 mm have no significant thermal performances, it can be deduced that 7-mm wire pitch is the optimum condition again from both practical and economical aspects.

Using the simulation results in **Figure 10**, the wire efficiency can also be calculated. Overall, increasing the inlet mass flow also improves the wire efficiency. Nonetheless, the maximum efficiency is reached for the inlet mass flow of $0.57 \times 10^{-3} \text{ kg s}^{-1}$ irrespective of the wire pitch. The wire pitch in woven matrix configuration affects the wire efficiency, and it is found that 7-mm wire pitch yields the highest efficiency of 73% at the inlet mass flow of $0.57 \times 10^{-3} \text{ kg s}^{-1}$ which is consistent with the above discussion.

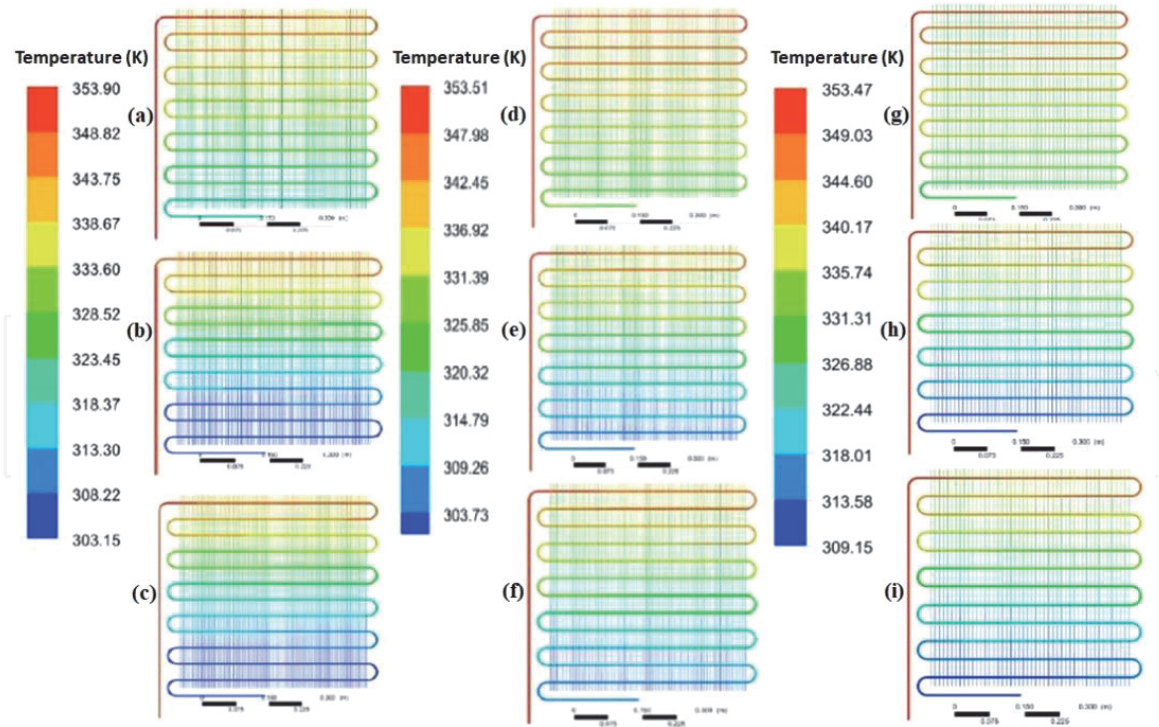


Figure 10.

Temperature profile of single woven matrix wire and tube heat exchanger bearing pitch wire of (a–c) 5 mm, (d–f) 7 mm, and (g–i) 9 mm operated using the inlet mass flow of (top) $1.10 \times 10^{-3} \text{ kg s}^{-1}$, (middle) $0.57 \times 10^{-3} \text{ kg s}^{-1}$, and (bottom) $0.55 \times 10^{-3} \text{ kg s}^{-1}$. Figures from Ref. [27] used with permission.

6. Conclusion

In this chapter, we have discussed that geometrical design along with optimum operating condition substantially control the overall performance of wire and tube heat exchanger. It has been demonstrated that for the commonly used inline wire and tube heat exchanger the efficiency can be predicted using the empirical formula (logarithmic function), which depends merely on the geometrical aspect (wire pitch to wire length ratio) and the Rayleigh number. Consistent with the heat transfer theory in a practical heat exchanger increasing the inlet fluid temperature and slowing down the mass flow rate typically yield higher-heat exchanger capacity and efficiency irrespective of the wire-tube configuration, including the inline, single-staggered, and woven matrix. Nonetheless, among the three investigated wire-tube configurations the single-staggered wire and tube heat exchanger is promising as the most efficient heat exchanger by taking into account the overall thermal performance, material mass, and cost for manufacturing.

This chapter also presents a numerical model based on the finite element method (FEM) that has been developed to evaluate and optimize the geometrical design of a single-staggered wire and tube heat exchanger with the optimization constraints of wire pitch and wire diameter. The FEM has successfully modeled the thermal behavior of the heat exchanger, which is validated by the experimental data showing an average numerical error of less than 5%. To understand the underlying phenomena in the heat transfer process, computational fluid dynamics (CFD) analysis enables the discussion of the local and near-surface airflow affecting the natural convection mechanism, and the heat flux on the outer wire-tube surfaces, which is responsible for the radiation from the surface to the surrounding environment. In addition, CFD analysis alone also allows for a comprehensive analysis of wire and tube heat exchanger running at certain operating conditions, and eventually, the

heat exchanger capacity as well as the heat exchanger efficiency can be calculated based on the simulation results.

Acknowledgements

Financial support by the Center of Research and Development (*Lembaga Penelitian dan Pengabdian Kepada Masyarakat*) of Universitas Negeri Surabaya and the directorate of research and community development (*Direktorat Riset dan Pengabdian Kepada Masyarakat*) of Institut Teknologi Sepuluh Nopember is highly acknowledged. Authors also would like to thank to the heat transfer laboratory of Universitas Negeri Surabaya for their technical support.

Conflict of interest

The authors declare that there is no conflict of interest.

Nomenclature

A	area (m ²)
C _p	specific heat of hot and cold fluid (J/kg K)
C	heat exchanger capacity (W/kg)
D	diameter (m)
<i>f</i>	optimization factor
g	acceleration of gravity (9.8 m/s ²)
GP	geometrical parameter
Gr	Grashof number
<i>h</i>	heat transfer coefficient (W/m ² K)
H	height of heat exchanger (m)
<i>k</i>	conduction heat transfer coefficient (W/m K)
L	length (m)
<i>m</i>	mass flow rate, (kg/s)
Nu	Nusselt number
p	pitch distance (m)
Pr	Prandtl number
Q	heat transfer rate (W)
<i>r</i>	radius (m)
R	heat resistance (K/W)
Ra	Rayleigh number
s	spacing (m)
T	temperature, °C or K
W	heat exchanger width (m)
ϵ	heat exchanger effectiveness, n.d

Subscripts

el	refers to element of finite element model
f	refers to fluid
i,o	refers to inner and outer surface
in, out	refers to inlet flows and outlet flows

max	refers to maximum condition
s	refers to surface of the wire tube
t	refers to tube
w	refers to wire
x	refers to position at x direction
∞	refers to ambient/surrounding air

Greek symbols

α	thermal diffusivity (m^2/s)
β	thermal expansion coefficient (K^{-1})
θ	polar or cone angle measured from normal of surface, rad.
ρ_f	density of a fluid (kg/m^3)
σ	Stefan-Boltzmann constant
ν	kinetic viscosity (m^2/s)

Author details

I Made Arsana^{1*} and Ruri Agung Wahyuono^{2,3}

1 Faculty of Engineering, Universitas Negeri Surabaya, Department of Mechanical Engineering, Surabaya, East Java, Indonesia

2 Faculty of Industrial Technology and System Engineering, Department of Engineering Physics, Institut Teknologi Sepuluh Nopember, Surabaya, Indonesia

3 ENABLE Work Group, Laboratory of Advanced Functional Materials, Faculty of Industrial Technology and System Engineering, Department of Engineering Physics, Institut Teknologi Sepuluh Nopember, Surabaya, Indonesia

*Address all correspondence to: madearsana@unesa.ac.id

IntechOpen

© 2021 The Author(s). Licensee IntechOpen. This chapter is distributed under the terms of the Creative Commons Attribution License (<http://creativecommons.org/licenses/by/3.0>), which permits unrestricted use, distribution, and reproduction in any medium, provided the original work is properly cited. 

References

- [1] Lum JMS, Clausing AM. An Investigation of the Air-Side Forced Convection Heat Transfer from Saw-Tooth Shaped, Multi-Layer, Wire-on-Tube Condensers. Reports. Urbana: Air Conditioning and Refrigeration Center, University of Illinois; 1997
- [2] Hoke JL, Swofford TD, Clausing AM. An Experimental Investigation of the Air-Side Convective Heat Transfer Coefficient on Wire and Tube Refrigerator Condenser Coils. Reports. Urbana: Air Conditioning and Refrigeration Center, University of Illinois; 1995
- [3] da Silva R, Melo EC. A Correlation for the air-side heat transfer coefficient of natural-draft wire-on-tube condensers. Articles in the Research Laboratories for Emerging Technologies in Cooling and Thermophysics. 2019. Available from: <https://polo.ufsc.br/publicacoes/a-correlation-for-the-air-side-heat-transfer-coefficient-of-natural-draft-wire-on-tube-condensers.html>
- [4] Arsana IM, Wahyuono RA. Chapter: Nanofluid-Enhancing Shell and Tube Heat Exchanger Effectiveness with Modified Baffle Architecture. In: Miguel Araiz, editor. Heat Transfer-Design, Experimentation and Applications. UK: IntechOpen; pp. 95. DOI: 10.5772/intechopen.96996
- [5] Arsana IM, Muhimmah LC, Nugroho G, Wahyuono RA. Enhanced heat transfer effectiveness using low concentration SiO₂-TiO₂ core-shell nanofluid in a water/ethylene glycol mixture. Journal of Engineering Physics and Thermophysics. 2021;94:423-430. DOI: 10.1007/s10891-021-02312-x
- [6] Witzell OW, Fontaine WE. What are the heat transfer characteristics of wire and tube condensers? Refrigerating Engineering. 1957;65:33-37
- [7] Witzell OW, Fontaine WE. Design of wire and tube condensers. Refrigerating Engineering. 1957;65:41-44
- [8] Tagliafico L, Tanda G. Radiation and natural convection heat transfer from wire-and-tube heat exchangers in refrigeration appliances. International Journal of Refrigeration. 1997;20(7): 461-469
- [9] Lee T-H, Yun J-Y, Lee J-S, Park J-J, Lee K-S. Determination of airside heat transfer coefficient on wire-on-tube type heat exchanger. International Journal of Heat and Mass Transfer. 2001;44:1767-1776
- [10] Espíndola RS, Boeng J, Knabben FT, Hermes CJL. A new heat transfer correlation for natural draft wire-on-tube condensers for a broad geometry span. International Journal of Refrigeration. 2020;114:10-18. DOI: 10.1016/j.ijrefrig.2020.02.025
- [11] Badwar SR, Joshi M, Mandale S, Kujur A. Experimentation and performance analysis of natural draft wire on tube condenser. International Journal of Recent Technology and Engineering. 2019;8(3):4303-4308. DOI: 10.35940/ijrte.C5174.098319
- [12] Belman-Flores JM, Heredia-Aricapa Y, Garcia-Pabón JJ, Gallegos-Munoz A, Serrano-Arellano J, Pérez-Reguera CG. An approximate model of a multilayer wire-on-tube condenser operating with R134a and R600a: Experimental validation and parametric analysis. Case Studies in Thermal Engineering. 2021;25:100927. DOI: 10.1016/j.csite.2021.100927
- [13] Nuntaphan A, Vithayasai S, Vorayos N, Vorayos N, Kiatsiriroat T. Use of oscillating heat pipe technique as extended surface in wire-on-tube heat exchange for heat transfer enhancement. International

Communications in Heat and Mass Transfer. 2010;**37**:287-292. DOI: 10.1016/j.icheatmasstransfer.2009.11.006

[14] Choi SH, Cho WH, Kim JW, Kim JS. A study on the development of the wire woven heat exchanger using small diameter tubes. *Experimental Thermal and Fluid Science*. 2004;**28**:153-158. DOI: 10.1016/80894-1777(03)00034-7

[15] Kushwah A, Pandey KD, Gupta A, Saxena G. Thermal modeling of heat exchanger: A review. *International Journal of Advance Research in Engineering, Science and Technology*. 2017;**4**(1):30-35

[16] Bansal PK, Chin TC. Modelling and optimisation of wire-and-tube condenser. *International Journal of Refrigeration*. 2003;**26**:601-613

[17] Gholap AK, Khan JA. Design and multi-objective optimization of heat exchangers for refrigerators. *Applied Energy*. 2007;**84**:1226-1239. DOI: 10.1016/j.apenergy.2007.02.014

[18] Quadir GA, Krishnan GM, Seetharamu KN. Modeling of wire-on-tube heat exchangers using finite element method. *Finite Elements in Analysis and Design*. 2002;**38**:417-434. DOI: 10.1016/S0168-874X(01)00079-8

[19] Imran AA, Jafal HM. Numerical modeling of wire and tube condenser used in domestic refrigerators. *Journal of Engineering and Development*. 2009; **13**(2):1-16

[20] Hadi SL, Arsana IM. Design and fabrication of woven matrix wire and tube heat exchanger [in Bahasa Indonesia]. *Jurnal Rekayasa Mesin*. 2014;**01**(03):56-63

[21] Putra TD, Arsana IM. Instrumentation system design for efficiency test in the wire and tube heat exchanger [in Bahasa Indonesia]. *Jurnal Rekayasa Mesin*. 2014;**01**(02):16-22

[22] Fikri MUK, Arsana IM. The effect of mass flow rate in the free convection wire and tube heat exchanger [in Bahasa Indonesia]. *Jurnal Teknik Mesin*. 2013; **01**(02):71-79

[23] Agung DP, Arsana IM. The effect inlet temperature in the free convection wire and tube heat exchanger [in Bahasa Indonesia]. *Jurnal Teknik Mesin*. 2013; **01**(02):80-85

[24] Arsana IM, Budhikardjono K, Susianto AA. Modelling of the single staggered wire and tube heat exchanger. *International Journal of Applied Engineering Research*. 2016;**11**(8): 5591-5599. DOI: 10.1051/mateconf/20165801017

[25] Arsana IM, Susianto BK, Altway A. Optimization of the single staggered wire and tube heat exchanger. *MATEC Web of Conferences*. 2016;**58**:01017. DOI: 10.1051/mateconf/20165801017

[26] Akbar FR, Arsana IM. Effect of wire pitch on capacity of single staggered wire and tube heat exchanger using computational fluid dynamic simulation. *International Journal of Engineering Transactions B: Applications*. 2020;**33**(8):1637-1642. DOI: 10.5829/ije.2020.33.08b.22

[27] Arsana IM, Rahardjo MAH. Simulation study on efficiency of woven matrix wire and tube heat exchanger. *International Journal of Engineering Transactions C: Aspects*. 2020;**33**(12): 2572-2577. DOI: 10.5829/ije.2020.33.12c.19

[28] Arsana IM. Empirical correlation of the free convection wire and tube heat exchanger efficiency [in Bahasa Indonesia]. *Proceeding of National Postgraduate Seminar*. 2002;01: C9-1-C9-5